Femtosecond x-rays from Thomson scattering using laser wakefield accelerators

INSTITUTE OF PHYSICS PUBLISHING MEASUREMENT SCIENCE AND TECHNOLOGY
Meas. Sci. Technol. **12** (2001) 1828–1834 PII: S0957-0233(01)23310-4

Femtosecond x-rays from Thomson scattering using laser wakefield accelerators

P Catravas, E Esarey and W P Leemans

Center for Beam Physics, Accelerator and Fusion Research Division,
Ernest Orlando Lawrence Berkeley National Laboratory, One Cyclotron Road,
University of California, Berkeley, CA 94720, USA

Received 23 March 2001, accepted for publication 5 June 2001
Published 9 October 2001
Online at stacks.iop.org/MST/12/1828

Abstract
The possibility of producing femtosecond x-rays through Thomson scattering high power laser beams off laser wakefield generated relativistic electron beams is discussed. The electron beams are produced with either a self-modulated laser wakefield accelerator (SM-LWFA) or through a standard laser wakefield accelerator (LWFA) with optical injection. For an SM-LWFA (LWFA) produced electron beam, a broad (narrow) energy distribution is assumed, resulting in x-ray spectra that are broadband (monochromatic). Designs are presented for 3–100 fs x-ray pulses and the expected flux and brightness of these sources are compared.

Keywords: x-ray, femtosecond, laser, electron beam, Thomson scattering, diffraction, laser wakefield acceleration

(Some figures in this article are in colour only in the electronic version; see `www.iop.org`)

1. Introduction

There are many different approaches to the generation of femtosecond x-ray pulses [1], one of them being Thomson scattering (TS) [2] an intense laser off an intense electron beam [3–15]. The first demonstration of the generation of sub-picosecond duration x-ray pulses using 90° TS was implemented at the Beam Test Facility of the Advanced Light Source at Lawrence Berkeley National Laboratory (LBNL) [7–9]. The generated x-ray pulse duration of 300 fs (FWHM) was determined by the convolution between the laser pulse duration (100 fs) and the crossing time of the laser across the tightly focused electron beam (200–250 fs). The number of x-rays and peak brightness of the 90° TS source experiments at LBNL was in part limited by the fact that the laser beam only interacted with about a 100 fs long electron beam slice (or 0.3% of all the available electrons), as well as the relatively high transverse emittance of the electron beam and low peak laser power used in the experiment. To increase the photon yield and source brightness, high quality femtosecond electron bunches are needed. Such electron bunches could then be used to produce femtosecond x-rays through 180° laser backscattering or through bremsstrahlung in a thin, solid target [15].

In this paper, we discuss the use of electron beams produced with laser wakefield accelerators (LWFAs) [16] for TS sources. The characteristic scale length of the accelerating field in a plasma-based accelerator [16] is the plasma wavelength, λ_p [m] $\simeq 3.3 \times 10^4 n_p^{-1/2}$ [cm^{-3}], where n_p is the plasma density. In the self-modulated laser wakefield accelerator (SM-LWFA) [17, 18], energies up to 100 MeV have been demonstrated in several experiments [19–27]. However, the energy spread is large (100%), since electrons from the background plasma are self-trapped in the accelerating fields of the wake. In the standard LWFA (typically $\lambda_p \sim 100\ \mu$m), electrons are not self-trapped and the production of electron beams with low momentum spread and good pulse-to-pulse energy stability requires femtosecond electron bunches to be injected with femtosecond synchronization with respect to the plasma wake. Although conventional electron sources (photocathode or thermionic RF guns) have achieved sub-picosecond electron bunches, the requirements for injection into plasma-based accelerators are presently beyond the performance of these conventional electron sources. Novel schemes which rely on laser triggered injection of plasma electrons into their own plasma wake have been proposed to generate the required femtosecond electron bunches [28–32].

We present designs of two novel sources of ultrashort x-ray pulses using TS from relativistic electron beams produced with LWFAs. In section 2, analytic expressions for TS including broadening from an arbitrary energy distribution are presented. These expressions are valid when the number of laser periods in the interaction region is large and provide a new and efficient way to evaluate the broadened spectral flux density for the wide range of possible energy distributions which LWFAs can produce. The limiting case of a narrow Gaussian distribution is shown to agree with standard formulae, and the analysis is applied in the case of 100% energy spread, where standard formulae do not apply. In section 3, TS designs using electron bunches produced via the SM-LWFA and a standard LWFA with optical injection are compared. The SM-LWFA yields large amounts of charge having large energy spread due to the uncontrolled trapping, and can provide x-ray flux over a large BW in a <100 fs pulse. The colliding pulse all-optical injector [28–30], which utilizes optical methods for triggering the trapping of electrons, holds the promise to produce low emittance electron bunches with low energy spread, which can be used to generate high brightness x-ray pulses with a few fs pulse length.

2. TS spectrum for arbitrary energy distribution

In general, the computation of spectral flux density from an electron beam, including realistic spreads in beam parameters, is performed through convolution of the electron distribution with the single electron spectral flux density. For a normalized electron distribution function, $f(\gamma, \theta_e)$, the resulting spectral flux density of the TS radiation from an electron beam is given by

$$\frac{\mathrm{d}^2 I_T}{\mathrm{d}\omega\,\mathrm{d}\Omega}(\theta,\omega) = \int \mathrm{d}\theta_e\,\mathrm{d}\gamma f(\theta_e,\gamma)\frac{\mathrm{d}^2 I}{\mathrm{d}\omega\,\mathrm{d}\Omega}(\theta-\theta_e,\gamma,\omega) \quad (1)$$

where $\mathrm{d}^2 I(\theta,\gamma,\omega)/\mathrm{d}\omega\,\mathrm{d}\Omega$ is the energy radiated by a single electron per unit frequency and solid angle, θ is the observation angle with respect to the longitudinal axis, ω is the frequency of the TS radiation, θ_e is the angle of the electron trajectory with respect to the longitudinal axis ($\theta_e^2 \ll 1$ is assumed) and γ is the electron energy.

The electron beams generated by different LWFA designs under current development exhibit strongly contrasting inhomogeneous broadening characteristics. When the electron energy distribution is narrow, standard formulae [3–9, 15] can be used to evaluate the contribution of energy spread to figures of merit such as the on-axis flux and brightness. Such is the case for the colliding pulse optical injection scheme [28, 29] in the standard LWFA. However, when the energy distribution is broad, such as for the SM-LWFA, the standard formulae cannot be applied. They become inapplicable because the on-axis frequency, $4\gamma^2\omega_0$, ($a_0 \ll 1, \theta = 0$) can change by up to three orders of magnitude across the energy distribution, accompanied by a factor of 30 change in the on-axis opening angle, $1/(\gamma\sqrt{N_0})$. Here, $a_0 \simeq 8.5 \times 10^{-10}\lambda_0\,[\mu\mathrm{m}]\,I^{1/2}\,[\mathrm{W\,cm^{-2}}]$ is the normalized vector potential of the laser pulse (laser strength parameter), I is the laser pulse intensity, λ_0 is the laser wavelength, $\omega_0 = 2\pi c/\lambda_0$ is the laser frequency and N_0 is the number of periods of the laser pulse with which the electron interacts. When a_0^2 is not small compared with unity, the situation is even more complex, as there is substantial overlap between harmonics radiated by the lower energy electrons of the distribution and radiation at the fundamental by higher energy electrons.

Computations which include arbitrary energy distributions can be simplified by noticing that a very large number of periods is available in the interaction region (up to 1000s) in TS designs, so that the intrinsic spectral line broadening at any fixed angle is essentially a delta function compared with the contribution from the energy distribution for realistic parameters. In this case, analytic expressions can be obtained for spectral flux density which are valid for any energy distribution.

2.1. Single electron spectrum

The general form of the energy radiated by a single electron per unit frequency, $\mathrm{d}\omega$, per unit solid angle, $\mathrm{d}\Omega$, derived by integrating the Liénard–Wiechert potentials, can be found in [4]. Here, we consider the small a_0 limit, $a_0^2 \ll 1$, where the main contribution to the radiation comes from the fundamental. For typical experimental parameters and regimes of interest, the electron beam energy satisfies $\gamma^2 \gg 1$ and the angle of observation is small ($\theta^2 \ll 1$). Then, the TS spectral flux density simplifies to

$$\frac{\mathrm{d}^2 I}{\mathrm{d}\omega\,\mathrm{d}\Omega} \simeq r_e mc\left(\frac{\omega}{4\gamma^2\omega_0}\right)^2 \gamma^2 N_0^2 a_0^2 R(\omega,\omega_0) \quad (2)$$

where $r_e = e^2/mc^2$ is the classical electron radius, m is the electron mass, c is the speed of light and the spectral flux density has been evaluated in the plane perpendicular to that of the laser polarization.

The resonance function, $R(\omega,\omega_0)$, determines many of the defining characteristics of Thomson scattered radiation:

$$R(\omega,\omega_0) = \left(\frac{\sin \bar{k}L/2}{\bar{k}L/2}\right)^2 \quad (3)$$

where

$$\bar{k} = k(1+\gamma^2\theta^2)/(4\gamma^2) - k_0 \quad (4)$$

$L = N_0\lambda_0$ is the length of the interaction region, $k = \omega/c$ is the radiation wavenumber and $k_0 = \omega_0/c$ is the laser wavenumber. The condition $\bar{k} = 0$ corresponds to a Doppler shifted resonant frequency of

$$\omega_r \simeq 4\gamma^2\omega_0/(1+\gamma^2\theta^2) \quad (5)$$

or, equivalently, a resonant energy of

$$\gamma_r^2 \simeq \frac{\omega/4\omega_0}{1-\omega\theta^2/4\omega_0}. \quad (6)$$

Of particular interest to TS using laser wakefield electron injectors is the behaviour for a large number of periods, N_0. In the limit $N_0 \to \infty$,

$$R \to \Delta\omega_r\delta(\omega-\omega_r) = \Delta\gamma_r\delta(\gamma-\gamma_r) \quad (7)$$

where $\Delta\omega_r = \omega_r/N_0$ is the spectral width, which corresponds to $\Delta\gamma_r = 2\gamma_r^3\omega_0/N_0\omega_r$.

2.2. Spectrum for the SM-LWFA bunch

To include the effect of energy spread, the spectral flux density is integrated over the electron energy spectrum, $f(\gamma)$,

$$\frac{\mathrm{d}^2 I_T}{\mathrm{d}\omega\,\mathrm{d}\Omega} \simeq \int \mathrm{d}\gamma f(\gamma) \frac{\mathrm{d}^2 I}{\mathrm{d}\omega\,\mathrm{d}\Omega}. \tag{8}$$

Beam emittance is neglected since the angular width of the spectrum over the photon energies of interest is much broader than typical beam divergences (see figure 2(c)). Assume $f(\gamma)$ is slowly varying compared to $R(\omega, \omega_r)$ for fixed ω. Integrating over the delta function approximation for $R(\omega, \omega_r)$ in frequency (energy) yields the following analytic form for the energy integrated spectrum:

$$\frac{\mathrm{d}^2 I_T}{\mathrm{d}\omega\,\mathrm{d}\Omega} \simeq \frac{r_e mc}{16} N_0 a_0^2 \left(\frac{\omega}{\omega_0}\right)^{3/2} f(\gamma = (\omega/4\omega_0)^{1/2}). \tag{9}$$

Of particular interest is the photon flux and brightness of the TS radiation. Assuming that the collection angle, θ_d, is small ($\theta_d < (\Delta\omega/\omega)^{1/2}/\gamma < (1/N)^{1/2}/\gamma$) so that the intensity distribution is flat over the solid angle $\Delta\Omega_d = \pi\theta_d^2$, the number of photons intercepted in a small bandwidth, $\Delta\omega$, and solid angle, $\Delta\Omega_d$, for an electron bunch with N_b electrons is

$$\begin{aligned} N_T &= \frac{N_b}{\hbar} \frac{\mathrm{d}^2 I_T}{\mathrm{d}\omega\,\mathrm{d}\Omega} \frac{\Delta\omega}{\omega} \pi\theta_d^2 \\ &\simeq \frac{\alpha_f}{16} N_b N_0 a_0^2 \left(\frac{\omega}{\omega_0}\right)^{3/2} f(\gamma = (\omega/4\omega_0)^{1/2}) \frac{\Delta\omega}{\omega} \pi\theta_d^2 \end{aligned} \tag{10}$$

where α_f is the fine structure constant. The average flux in photons per second, F_{av}, in the collection angle θ_d and with bandwidth $\Delta\omega$ is N_T multiplied by the repetition rate, f_{rep}, of the laser/electron beam, i.e., $F_{av} = N_T f_{rep}$. The average source brightness (in photons s^{-1} mm^{-2} mrad^{-2}/0.1% BW) is given by

$$\begin{aligned} B_{av} &= \frac{F_{av}}{(2\pi)^2 {r_b}^2 {\theta_d}^2} \\ &\simeq \frac{\alpha_f N_b N_0 a_0^2}{64\pi r_b^2} \left(\frac{\omega}{\omega_0}\right)^{3/2} f(\gamma = (\omega/4\omega_0)^{1/2}) \frac{\Delta\omega}{\omega} \end{aligned} \tag{11}$$

where r_b is the electron bunch radius. The peak flux and brightness are, respectively, $F_{pk} = F_{av}/(\tau_x f_{rep})$ and $B_{pk} = B_{av}/(\tau_x f_{rep})$, where τ_x is the x-ray pulse duration, which is assumed to be approximately equal to the electron bunch duration.

2.3. TS spectrum for narrow energy distribution

For an electron bunch with a narrow energy spread $\Delta\gamma/\gamma_0 \ll 1$ about a mean energy, γ_0, and for a narrow distribution in beam angle with spread $\Delta\theta = \epsilon_n/\gamma r_b \ll 1$, where ϵ_n is the normalized emittance and r_b the beam radius, estimates for flux and brightness have been derived [4, 27]. In particular, the total number of photons scattered per laser–electron bunch interaction into a small bandwidth, $\Delta\omega/\omega \ll 1$, is approximately

$$N_T = 2\pi\alpha N_0 a_0^2 \frac{\Delta\omega}{\omega} N_b F_{coll} \tag{12}$$

assuming $a_0^2 \ll 1$, where N_b is the number of electrons per bunch interacting with the laser pulse. Here, F_{coll} is a factor determined by the collection angle, θ_d, of the x-ray optics, i.e., $F_{coll} = \theta_d^2/(\theta_d^2 + \theta_T^2)$ with

$${\theta_T}^2 \simeq [(\Delta\omega/\omega)^2 + (\Delta\omega/\omega)_0{}^2 + (\Delta\omega/\omega)_\epsilon{}^2 + (\Delta\omega/\omega)_i{}^2]^{1/2}/\gamma^2 \tag{13}$$

where $(\Delta\omega/\omega)_0 = 1/N_0$, $(\Delta\omega/\omega)_\epsilon = {\epsilon_n}^2/{r_b}^2$ and $(\Delta\omega/\omega)_i = 2\Delta\gamma/\gamma$ represent the contributions to the bandwidth from the finite interaction length, the beam emittance and energy spread, respectively. The average flux is $F_{av} = N_T f_{rep}$ and the average brightness is

$$B_{av} = \frac{N_T f_{rep}}{(2\pi)^2 \sigma_r^2 \sigma_\theta^2} \tag{14}$$

where $\sigma_r \simeq r_b$ and $\sigma_\theta \simeq \theta_T$ are the rms source size and opening angle of the radiation, respectively, and $r_b \simeq r_0$ has been assumed, where r_0 is the laser pulse radius.

3. Examples based on LWFAs

3.1. Self-modulated laser wakefield accelerator

The SM-LWFA provides short (<100 fs), high charge (>10^{10} electrons) bunches having a broad energy distribution. Thus TS using an SM-LWFA injector will be characterized by high photon flux with broad bandwidth. In the SM-LWFA, an instability initiated at the front of a laser pulse leads to increasingly strong self-modulation of the laser pulse envelope at λ_p periodicity and resonant enhancement of the wakefield. The requirements for this instability are a laser pulse long compared with λ_p and powers exceeding the threshold for relativistic self-focusing. The strong enhancement of wakefield strength over the standard LWFA leads to self-trapping of plasma electrons, while the relativistic focusing increases the acceleration distance, allowing high electron energies to be reached with a high charge per bunch. Bunch lengthening due to space charge effects [33] can be avoided by minimizing the propagation distance of the electron bunch before the TS interaction, thus keeping the electron bunch length as close as possible to the laser pulse length. Shorter drive pulse lengths combined with higher plasma densities can lead to higher x-ray brightness and shorter electron beam bunch lengths. That is, decreasing the laser pulse length $L = c\tau_L$ requires increasing plasma density to satisfy $L > \lambda_p$, and the wake axial electric field scales roughly as $E_z \sim \sqrt{n_p}$, where n_p is the plasma density. Uncontrolled trapping leads to an energy distribution of the form [21–27]

$$f(\gamma) = f_0 \exp(-\gamma/\gamma_0) \tag{15}$$

where f_0 and γ_0 are constants.

Empirical parameters for the LBNL SM-LWFA are as follows [27]. The normalized electron distribution, measured with a bending magnet, is

$$f(\gamma) = 0.24\,\mathrm{e}^{-0.15\gamma}. \tag{16}$$

The total charge is at least 5 nC per bunch, or 3×10^{10} particles, and is generated with a driving pulse of 50 fs with $a_0 \sim 1$ at 10 Hz and a plasma density of a few 10^{19} cm^{-3}.

Using these electron beam parameters, the following TS source may be designed. A 600 mJ, 1.4 ps laser pulse with

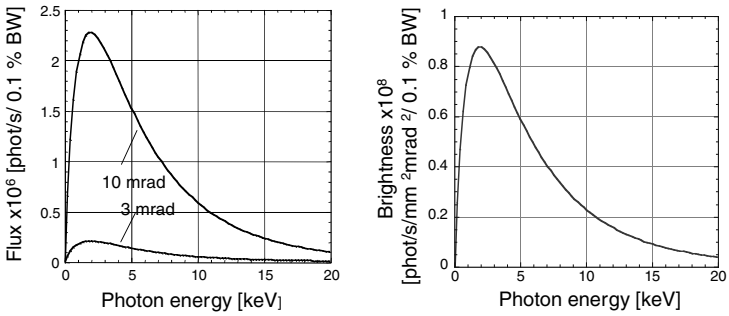

Figure 1. The average flux into 3 and 10 mrad collection angles and average brightness for the SM-LWFA-based TS design (see table 1, column 2 for parameters) shows the influence of the high charge per bunch (∼5 nC) and broad energy distribution.

Table 1. Comparison of Thomson scattering source designs using laser wakefield accelerators and experimental results with an RF accelerator.

Parameter	Colliding pulse	SM-LWFA	BTF [7–9]
Laser wavelength λ_L [μm]	0.8	0.8	0.8
Laser pulse energy U_L [J]	0.5	0.6	0.04
Laser pulse duration (FWHM) [ps] τ_L	1	1.4	0.1
Electron beam energy γ	50	Exponential distribution	98
Number of electrons N_b	3×10^7	3×10^{10}	8×10^9
Electron bunchlength (FWHM) τ_b [ps]	0.003	0.1	30
Electron spot size (FWHM) r_b [μm]	6	6	90
Normalized emittance ϵ_N [mm mrad]	1	1	30
Bandwidth $\delta\omega/\omega$	10^{-3}	10^{-3}	10^{-3}
Collection angle [mrad]	1	3	1
Repetition rate [Hz]	10	10	2
Flux (ph s^{-1}/0.1% BW) in collection angle	5×10^4	2×10^5	6×10^2
Ave. brightness (ps s^{-1} mm^{-2} mrad^{-2}/0.1% BW)	1.5×10^8	9×10^7	3×10^3
Peak brightness (ps s^{-1} mm^{-2} mrad^{-2}/0.1% BW)	5×10^{21}	10^{20}	10^{16}
Total number of photons s^{-1} (all frequencies, all angles)	2×10^8	3×10^{11}	2×10^7
X-ray pulselength [fs]	3	<100	300
X-ray photon energy [keV]	12.4	Broadband, max at 2–3 keV	30

a wavelength of 800 nm and a repetition rate of 10 Hz is focused to a spot size of 6 microns. With a corresponding a_0 of 0.7, about 3×10^{11} photons per second are radiated in all frequencies and all angles. Brightness as a function of photon energy in photons s^{-1} mm^{-2} mrad^{-2}/0.1% BW at a 10 Hz repetition rate, calculated with equation (11), is shown in figure 1. The average brightness for these parameters peaks between 2 and 3 keV and has a total bandwidth of about 10 keV. As the result of the use of an ultrashort laser pulse, the peak brightness ($B_{pk} = B_{av}/(\tau_x f_{rep}) \sim 3$–$4 \times 10^{19}$ photons s^{-1} mm^{-2} mrad^{-2}/0.1% BW) is 12 orders of magnitude higher than the average brightness for these parameters. The parameters and x-ray characteristics are summarized in table 1, column 2.

The electron energy distribution and the angular density of the spectral flux over a range of 20 keV in photon energy and 50 mrad observation angle, in photons per second per 0.1% BW per solid angle, are shown in figures 2(a) and 2(c), using a generalization of equation (11) to account for off-axis angles. The higher the on-axis photon energy corresponding to each slice in energy the lower the amplitude. Beam emittance is about 1 π mm mrad. Note that for the corresponding divergences of ∼10 mrad, divergence broadening can be neglected for the bulk of the emissions (photon energies less than 15 keV).

3.2. Colliding pulse all-optical injector

In this section, we discuss the generation of near-monochromatic x-rays using TS off electron bunches produced with the colliding pulse laser-plasma electron source for generating truly femtosecond electron bunches [28–30]. The source generates ultrashort electron bunches by using laser pulses to dephase background plasma electrons undergoing fluid oscillations in a standard LWFA plasma wake. The colliding pulse scheme has the ability to produce femtosecond electron bunches with low fractional energy spreads using relatively low injection laser pulse intensities compared to the pump laser pulse. ($a_{inj}^2 \ll a_{pump}^2 \sim 1$, where $a = eA/mc^2$ is the normalized vector potential of the pulse).

The colliding pulse optical injection scheme employs three short laser pulses: an intense ($a_0^2 \simeq 1$) pulse (denoted by subscript 0) for plasma wake generation, a forward going injection pulse (subscript 1) and a backward going injection pulse (subscript 2). The frequency, wavenumber and normalized intensity are denoted by ω_i, k_i and a_i ($i = 0, 1, 2$). Furthermore, $\omega_1 = \omega_0$, $\omega_2 = \omega_0 - \Delta\omega$ ($\Delta\omega \geqslant 0$) and $\omega_0 \gg \Delta\omega \gg \omega_p$ are assumed such that $k_1 = k_0$, and $k_2 \simeq -k_0$. The pump pulse generates a plasma wake with phase velocity near the speed of light ($v_{p0} \simeq c$). When the injection pulses collide (some distance behind the pump) they generate a slow ponderomotive beat wave with a phase velocity $v_{pb} \simeq \Delta\omega/2k_0 \ll c$. During the time in which the two

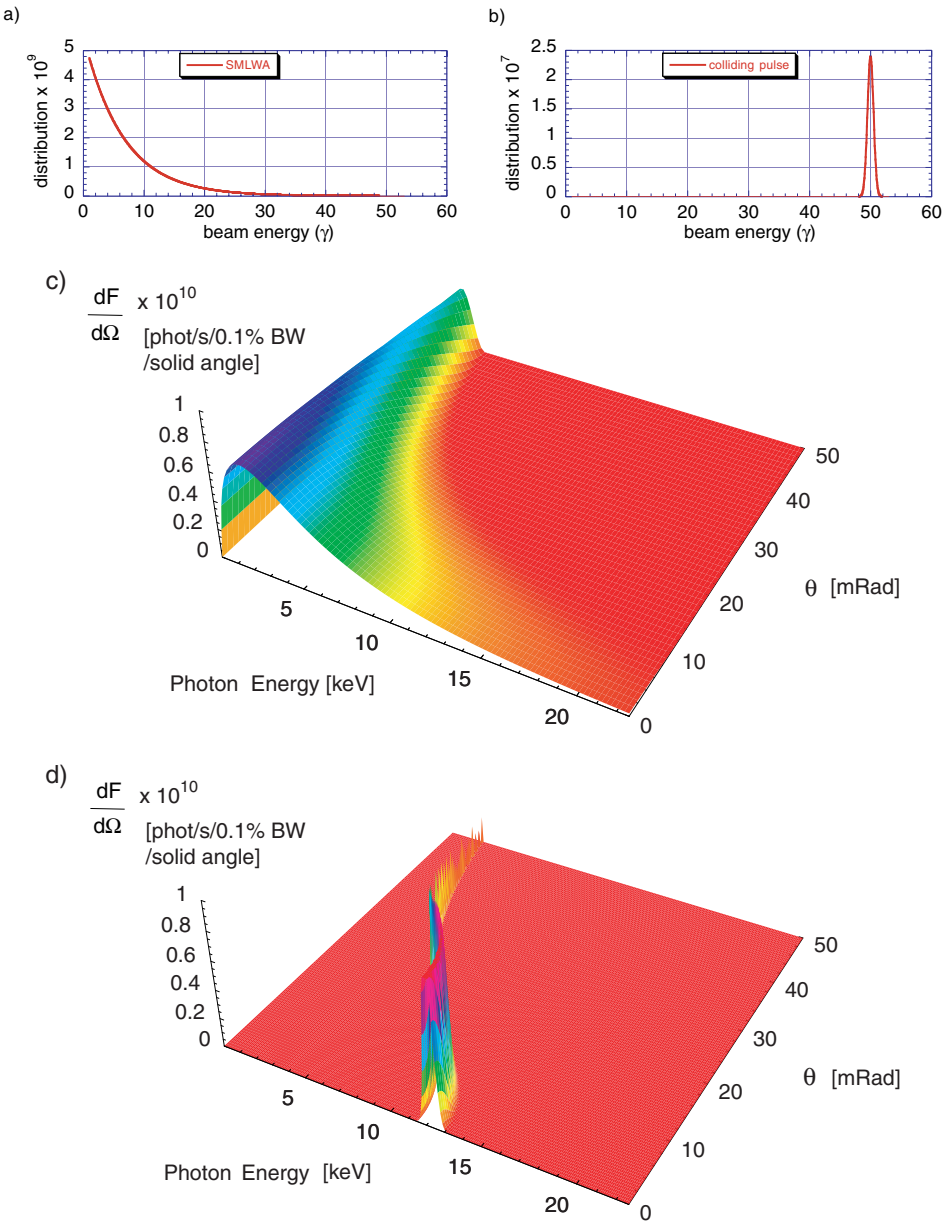

Figure 2. For the parameters listed in table 1, the corresponding energy distribution and spectral flux density, $\mathrm{d}F/\mathrm{d}\Omega$, in photons per second per 0.1% BW per solid angle, are shown in (a) and (c), respectively, for SM-LWFA and in (b) and (d) for colliding pulses. The integral of the distributions are 3×10^{10} electrons per bunch for SM-LWFA and 3×10^{7} electrons per bunch for colliding pulses. The intensity distributions illustrate the contrast between the two injection schemes in scattered x-ray bandwidth and spatial collimation at a fixed observation frequency.

injection pulses overlap, a two-stage acceleration process can occur, i.e., the slow beat wave injects plasma electrons into the fast wakefield for acceleration to high energies.

Injection and acceleration can occur at low densities ($\lambda_p/\lambda \sim 100$), thus allowing for high single-stage energy gains, with normalized injection pulse intensities of $a_1 \sim a_2 \sim 0.2$. Furthermore, the colliding pulse concept offers detailed control of the injection process: the injection phase can be controlled via the position of the forward injection pulse, the beat phase velocity via $\Delta\omega$, the injection energy via the pulse amplitudes and the injection time (number of trapped electrons) via the backward pulse duration. Estimates indicate that space charge effects can be neglected while the bunch remains inside the plasma [29] and can be minimized for sufficiently high energy electron beams [33].

In the TS example summarized in column 1 of table 1, a 0.8 micron laser with 500 mJ energy and 1 ps duration focused to a 6 micron spot is scattered off of a 25 MeV electron beam with a few fs bunch length.

Electron beam parameters from simulations discussed in the previous section are used, and the design on-axis photon energy is 12.4 keV. For a repetition rate of 10 Hz and a 1 mrad collection angle, the average brightness is about 10^8 photons s^{-1} mm^{-2} $\mathrm{mrad}^{-2}/0.1\%$ BW. Due to the low contributions of inhomogeneous broadening, the peak brightness of 5×10^{21} photons s^{-1} mm^{-2} $\mathrm{mrad}^{-2}/0.1\%$ BW is

two orders of magnitude higher than for the SM-LWFA in spite of three orders of magnitude lower total flux into all angles and frequencies. From this example, we conclude that this unique source, capable of producing truly femtosecond pulses, should have sufficient flux and brightness to perform pump–probe type experiments.

The full spatial and spectral characteristics are shown in figure 2(d), along with the energy distribution (figure 2(b)). The profile in figure 2(d) can be thought of as a composite slice of the SM-LWFA profile (figure 2(c)). The energy distribution for the SM-LWFA is similar to a weighted sum of narrow energy slices, and the topography of the spectral flux density of the SM-LWFA arises from a sum of weighted contributions similar to that of figure 2(d), each having a different on-axis frequency. Note also that because N_0 is large, the spectral flux density contains a clear signature of the energy distribution in both designs and can be used as a diagnostic.

4. Conclusion

Laser wakefield accelerators provide electron bunches suitable for the production of ultrashort, high brightness x-ray pulses through 180° Thomson scattering. To date the study of ultrafast processes has largely relied on femtosecond optical pulses from mode-locked lasers. Since x-rays interact with core electronic levels and hence are effective structural probes, the availability of femtosecond x-ray pulses and the intrinsic synchronization between laser and x-ray pulses would make it possible to directly probe changes in atomic structure on ultrafast time scales.

The self-modulated laser wakefield accelerator provides high charge (5 nC) in bunches of less than 100 fs at 100% energy spread (the bulk of the distribution is at energies of a couple of MeV with a exponential tail extending out to tens of MeV). The TS spectrum and spatial profile is characteristically broad. Based on current measured values for such electron bunches, a design having $a_0 < 1$ which sets the bulk of the photon energies in the range of a few keV has been described. Peak brightnesses are predicted to exceed 10^{19} photons s^{-1} mm^{-2} $mrad^{-2}$/0.1% BW.

The proposed colliding pulse optical injection scheme has the ability to produce electron bunches of a few fs, having low energy spread and emittance. While charge levels are lower than for the SM-LWFA, low energy spread and divergence enables an increase of two orders of magnitude in peak brightness.

Although summarizing source performance using a single number (i.e. peak brightness) can be useful for some applications, proper evaluation must be made based on the type of experiment and its requirements, as well as on the ease of implementation and available infrastructure. These laser-plasma electron beam sources offer some unique advantages: (1) TS based sources can produce tunable ultrashort x-ray pulses using relatively low energy electron beams. (2) The source parameters such as photon energy, brightness and bandwidth, are controllable through electron beam and laser parameters. For example, rapid polarization and wavelength control is possible through the laser polarization and wavelength tuning, respectively. (3) The pulse length is controllable through the laser pulse length, electron bunch length and interaction geometry. (4) The methods provide perfect synchronization between the laser pulse, electron bunch and x-ray pulse.

These laser-plasma sources of x-rays are of table-top size. The major equipment required for such a source is a high power, chirp-pulse amplification laser system, which is becoming commonplace [34]. However, for all laser-plasma sources, laser repetition rate and average power have been some of the main limitations. Future research into the development of high average power lasers, as well as optical storage cavities for ultra-short pulses, would have a tremendous impact on the scientific reach of these laser-plasma based sources.

Acknowledgment

This work was supported by the Department of Energy under contract No DE-AC-03-76SF0098.

References

[1] See, for example, Gauthier J C (ed) 2000 Special issue on new ultrafast x-ray sources and their applications *C. R. Acad. Sci. Paris* IV **1**
[2] Arutyumain F R and Tumanian V A 1963 *Phys. Lett.* **4** 173
Milburn R H 1963 *Phys. Rev. Lett.* **10** 75
Sarachik E S and Schappert G T 1970 *Phys. Rev.* D **1** 2738
[3] Sprangle P, Ting A, Esarey E and Fisher A 1992 *J. Appl. Phys.* **72** 5032
Sprangle P and Esarey E 1992 *Phys. Fluids* B **4** 2241
[4] Esarey E, Ride S K and Sprangle P 1993 *Phys. Rev.* E **48** 3003
[5] Ride S K, Esarey E and Baine M 1995 *Phys. Rev.* E **52** 5425
Esarey E, Ride S K, Baine M, Ting A and Sprangle P 1996 *Nucl. Instrum. Methods* A **375** 545
[6] Kim K J, Chattopadhyay S and Shank C V 1994 *Nucl. Instrum. Methods* A **341** 351
[7] Schoenlein R W, Leemans W P, Chin A H, Volfbeyn P, Glover T E, Balling P, Zolotorev M, Kim K J, Chattopadhyay S and Shank C V 1996 *Science* **274** 236
[8] Leemans W P, Schoenlein R W, Volfbeyn P, Chin A H, Glover T E, Balling P, Zolotorev M, Kim K J, Chattopadhyay S and Shank C V 1996 *Phys. Rev. Lett.* **77** 4182
[9] Leemans W P, Schoenlein R W, Volfbeyn P, Chin A H, Glover T E, Balling P Zolotorev M, Kim K J, Chattopadhyay S and Shank C V 1997 *IEEE J. Quantum Electron.* **33** 1925
[10] Ting A, Fischer R, Fisher A, Evans K, Burris R, Krall J, Esarey E and Sprangle P 1995 *J. Appl. Phys.* **78** 575
[11] Glotin F, Ortega J-M, Prazeres R, Devanz G and Marcouille O 1996 *Phys. Rev. Lett.* **77** 3130
[12] Carroll F E, Waters J W, Traeger R H, Mendenhall M H, Clark W-W and Brau C A 1999 *Proc. SPIE* **3614** 139
[13] Krafft G 1999 Jefferson Laboratory, private communication
[14] Pogorelsky I V *et al* 2000 *Phys. Rev. Spec. Topics Accel. Beams* **3** 090702
[15] Leemans W P, Chattopadhyay S, Esarey E, Zholents A, Zolotorev M, Chin A, Schoenlein R and Shank C V 2000 *C. R. Acad. Sci. Paris* IV **1** 279
[16] Esarey E, Sprangle P, Krall J and Ting A 1996 *IEEE Trans. Plasma Sci.* **24** 252
[17] Esarey E, Krall J and Sprangle P 1994 *Phys. Rev. Lett.* **72** 2887
[18] Esarey E, Sprangle P, Krall J and Ting A 1997 *J. Quantum Electron.* **33** 1879
[19] Modena A *et al* 1995 *Nature* **377** 606
[20] Nakajima K *et al* 1995 *Phys. Rev. Lett.* **74** 4428
[21] Umstadter D, Chen S-Y, Maksimchuk A, Mourou G and Wagner R 1996 *Science* **273** 472
Wagner R, Chen S Y, Maksimchuk A and Umstadter D 1997 *Phys. Rev. Lett.* **78** 3125

[22] Ting A, Moore C I, Krushelnick K, Manka C, Esarey E, Sprangle P, Hubbard R, Burris H R and Baine M 1997 *Phys. Plasmas* **4** 1889
Moore C, Ting A, Krushelnick K, Esarey E, Hubbard R F, Burris H R, Manka C and Sprangle P 1997 *Phys. Rev. Lett.* **79** 3909
[23] Gordon D *et al* 1998 *Phys. Rev. Lett.* **80** 2133
[24] Amiranoff F *et al* 1998 *Phys. Rev. Lett.* **81** 995
[25] Dorchies F *et al* 1999 *Phys. Plasmas* **6** 2903
[26] Santala M I K, Najmudin Z, Clark E L, Tatarakis M, Krushelnick K, Dangor A E, Malka V, Faure J, Allott R and Clarke R J 2001 *Phys. Rev. Lett.* **86** 1227
[27] Leemans W P, Rodgers D, Catravas P E, Geddes C G R, Fubiani G, Esarey E, Shadwick B A, Donahue R and Smith A 2001 *Phys. Plasmas* **8** 2510
[28] Esarey E, Hubbard R F, Leemans W P, Ting A and Sprangle P 1997 *Phys. Rev. Lett.* **79** 2682
[29] Schroeder C B, Lee P B, Wurtele J S, Esarey E and Leemans W P 1999 *Phys. Rev.* E **59** 6037
[30] Esarey E, Schroeder C B, Leemans W P and Hafizi B 1999 *Phys. Plasmas* **6** 2262
[31] Umstadter D, Kim J K and Dodd E 1996 *Phys. Rev. Lett.* **76** 2073
[32] Hemker R G, Tzeng K-C, Mori W B, Clayton C E and Katsouleas T 1998 *Phys. Rev.* E **57** 5920
[33] Fubiani G, Leemans W and Esarey E 2001 *Proc. Advanced Accelerator Workshop (Santa Fe, NM, 2000) (AIP Conf. Proc. vol 569)* p 423
[34] Mourou G A, Barty C P J and Perry M D 1998 *Phys. Today* **51** 22